Cathodoluminescence and transmission electron microscopy study of dark line defects in thick $In_{0.2}Ga_{0.8}As$/GaAs multiple quantum wells

D. H. Rich
Photonic Materials and Devices Laboratory, Department of Materials Science and Engineering, University of Southern California, Los Angeles, California 90089-0241

T. George, W. T. Pike, J. Maserjian, and F. J. Grunthaner
Center for Space Microelectronics Technology, Jet Propulsion Laboratory, California Institute of Technology, Pasadena, California 91109

A. Larsson
Chalmers University of Technology, Department of Optoelectronics and Electrical Measurements, S-412 96 Göteborg, Sweden

The spatial distribution of the long-wavelength luminescence in thick $In_{0.2}Ga_{0.8}As$/GaAs multiple quantum wells (MQWs) has been investigated using cathodoluminescence (CL) imaging and spectroscopy. The CL spectra show defect-induced broad bands between $1000 \lesssim \lambda \lesssim 1600$ nm. These bands exhibit spatial variations which correlate with the dark line defects (DLDs) observed in the $\lambda = 950$ nm exciton luminescence imaging. Transmission electron microscopy showed that [110]-oriented misfit dislocations occur primarily at the substrate-to-MQW and GaAs capping layer-to-MQW interfaces. The large spatial variation of the luminescence intensities indicates that the DLDs observed in CL images are caused by the presence of nonradiative recombination centers occurring in the MQW region located between the interface misfit dislocations. This study provides new information describing the origin and nature of DLDs and differs from previous models which have regarded the electronic nature of dislocation cores as the primary mechanism for inducing DLD radiative contrast in luminescence imaging of strained InGaAs/GaAs.

I. INTRODUCTION

There is considerable interest in utilizing the molecular beam epitaxial (MBE) growth of highly strained InGaAs/GaAs multiple quantum wells (MQWs) for photonic device applications, in the areas of optical computing, communication, and infrared detection. In particular, spatial light modulator (SLM) devices relying on photo- and electro-optic effects require uniform pixels of high-quality InGaAs/GaAs MQW layers grown on GaAs. Luminescence imaging studies of strained-layer systems have shown the existence of dark line defects (DLDs) related to the occurrence of dislocations which accommodate the lattice-mismatch strain when a critical thickness is exceeded.[1-4] Photoluminescence of thick single QWs of InGaAs/GaAs has shown the existence of longer-wavelength ($1000 \lesssim \lambda \lesssim 1600$ nm) luminescence features which were attributed to the presence of misfit dislocations at the InGaAs/GaAs interface.[5] In previous cathodoluminescence (CL) studies of strained III-V thin films, the radiative contrasts were believed to be caused by the electronic nature (i.e., dangling bonds and reconstruction) of the dislocation cores.[1,3] The present study examines an alternative explanation for the large radiative contrast seen in the CL imaging of dislocations. In the present article, we examine the spatial dependence of the luminescence in the $1000 \lesssim \lambda \lesssim 1600$ nm region using scanning CL imaging and spectroscopy. We show that these long-wavelength luminescence features correlate spatially with the DLDs seen in the imaging of the MQW exciton recombination at $\lambda \approx 950$ nm. Plan-view and cross-sectional transmission electron microscopy (TEM) show that misfit dislocations in the samples are confined to the region near the GaAs-to-MQW interfaces. The luminescence intensities from various MQW structures are quantified, and a large variation in intensity of the luminescence associated with the DLDs suggest that most of the QWs in the vicinity of the DLDs are affected by the misfit dislocations. This intensity variation is found to be relatively independent of the electron beam probing depth, and indicates that the QWs are affected homogeneously throughout all the layers, in contrast to the presence of misfit dislocations which occur *only* at the MQW-to-GaAs interfacial regions. This luminescence behavior is attributed to a relative increase in the number of *nonradiative* recombination centers occurring in MQW regions between the interface dislocations. These results suggest that nonradiative point defects in the MQW are left in the wake of dislocation propagation and multiplication. We demonstrate that a *Cottrell atmosphere* of point defects surrounding dislocations is the most reasonable explanation for the DLD behavior observed in this study of $In_{0.2}Ga_{0.8}As$/GaAs MQW structures. Similarly, in the Si system Kimerling and Patel,[6] using deep-level transient spectroscopy, have speculated that it is the point defects gettered around dislocations which are largely responsible for defect induced mid-gap states and the associated recombination properties. Our data is possibly the first which confirms the existence of this phenomenon in III-V materials.

II. EXPERIMENT

MQW samples were grown by MBE using standard In, Ga, and As sources. The present study involves 65-Å-thick $In_{0.2}Ga_{0.8}As$ quantum wells surrounded by GaAs barriers. In samples designated D92, D18, and D38, 44 periods of $In_{0.2}Ga_{0.8}As$ MQWs were grown with barrier thicknesses of 780, 400, and 115 Å, respectively. In sample D179, a 65 Å MQW structure having 100 and 1230 Å barriers with 14 periods (28 QWs) were grown. A control sample, D155, was grown with one 65-Å-thick QW. One of the samples, D92, was periodically δ doped; Be and Si doping planes with concentrations of 9.0×10^{12} and 3.0×10^{12} cm^{-2} were inserted at the centers and 290 Å off centers of the GaAs barriers to produce a *nipi* effect. This sample was grown originally for the purpose of studying suitable structures for optically addressed SLMs. The spatial separation of electrons and holes enables a large optically induced absorption modulation for this structure; this has been recently reported.[7,8] All samples were capped with a 5000 Å layer of undoped GaAs.

Cathodoluminescence measurements were performed with a JSM 840-F field emission scanning electron microscope (SEM). The optical collection system and sample cryogenic stage were designed and constructed at the Jet Propulsion Laboratory.[9] A North Coast E0-817L Ge *p-i-n* detector was used to measure the signal dispersed by a 0.25 m monochromator. An electron beam current of about 500 pA at varying accelerating voltages was used to probe the sample for the CL measurements. The sample was maintained at a temperature of ~77 K.

III. RESULTS AND DISCUSSION

Cross-sectional and plan view TEM measurements were performed on D38 and D18, two of the samples with the narrowest GaAs barriers in the 44 MQW structure, and they yielded similar results. Cross-sectional transmission electron microscope (TEM) images of D18 and D38 with the electron beam along the [110] azimuth is shown in Figs. 1(a) and 2, respectively. The MQW region shows well-ordered $In_{0.2}Ga_{0.8}As$ (dark lines) and GaAs (light lines) which are visibly free of structural defects (i.e., no misfit or threading dislocations are observed). The samples were examined over a length scale of ~100 μm, and only one typical image of each is presented in Figs. 1(a) and 2. In Fig. 2, arrows identifying individual misfit dislocations in D38 are shown. Only at the MQW-to-substrate interface and MQW-to-capping layer interface did there appear to be disorder in the form of interface misfit dislocations. Also, looping dislocations that have propagated into the GaAs substrate can be seen in Figs. 1(a) and 2. Various electron beam imaging conditions were used to image the cross-sectional slices of D18 and D38, and evidence of structural disorder in the MQW regions away from the interfaces was not found. Because of the long misfit dislocation segment length (greater than ~100 μm) and large strain-field gradients near misfit dislocations, we would expect to see misfit dislocations in the MQW region from our cross-sectional TEM analysis if they exist.
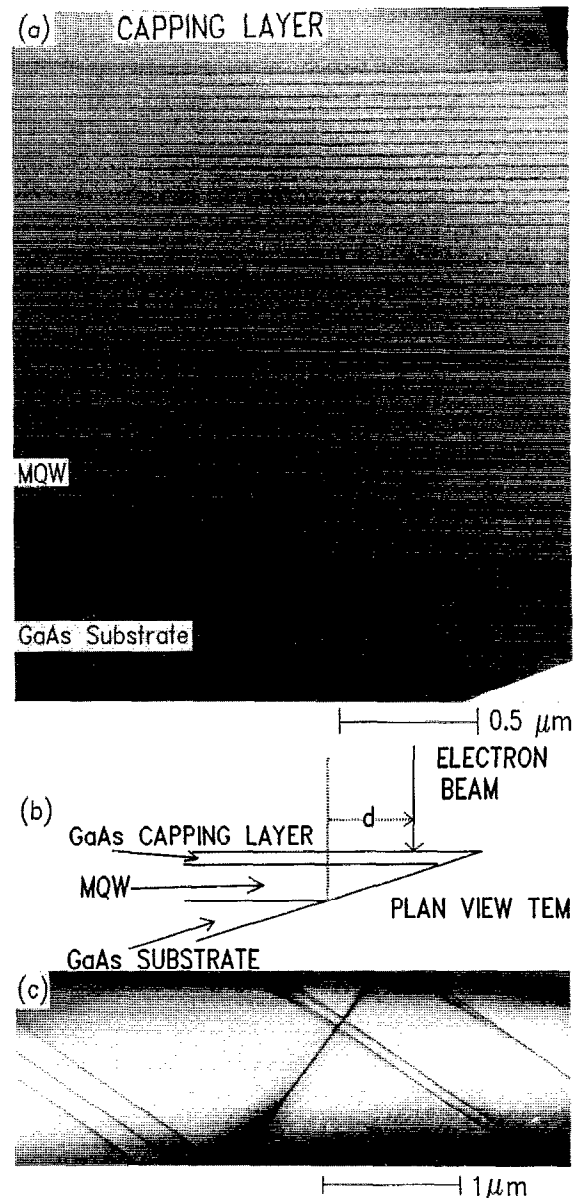

FIG. 1. Cross-sectional TEM image contrast of $In_{0.2}Ga_{0.8}As$/GaAs MQW sample D18 (a), plan-view TEM geometry showing thinning approach used to determine depth of misfit dislocation network (b), and plan-view TEM image of D18 (c).

In order to further examine this structure, plan-view TEM images were taken. The samples were mechanically thinned from the back side to produce a wedge-shaped edge, as illustrated in Fig. 1(b). TEM images were taken for various distances, *d*, along the surface of the sample. At a certain distance, a dark line network, as observed in the plan-view TEM image of sample D18 [see Fig. 1(c)], became visible. These dark lines represent contrast due to misfit dislocations which occur along both [110] directions as observed in previous studies off strained III-V materials employing TEM.[1,3,10,11] A Burgers vector analysis in plan-view TEM indicated these misfit dislocations were primarily of the 60° type. The depth at which the misfit dislocation network appeared was determined by *convergent beam*
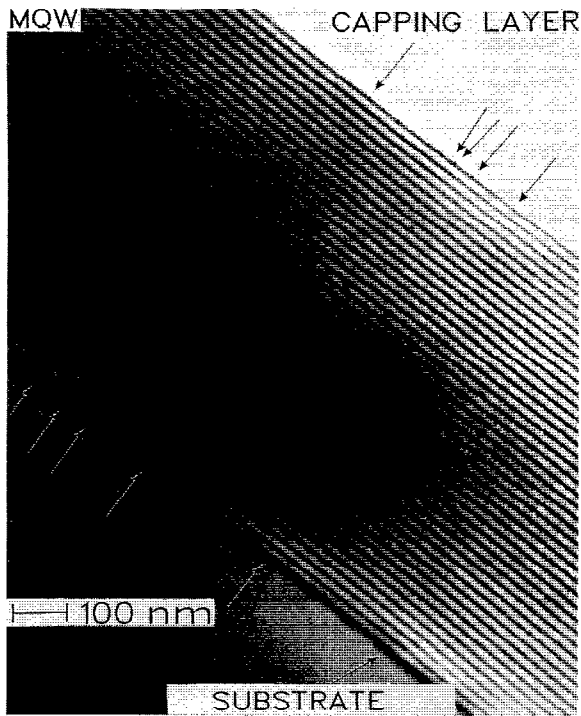
FIG. 2. Cross-sectional TEM image contrast of $In_{0.2}Ga_{0.8}As/GaAs$ MQW sample D38. The arrows point to misfit dislocations which occur at both the MQW-to-substrate and MQW-to-capping layer interfaces.

FIG. 3. Scanning monochromatic CL images of the e-hh exciton luminescence for $\lambda \sim 950$ nm. The sample number and MQW structure are described in (a)–(e). The 20 μm scale indicated in (a) also represents the scale for (b)–(d); note the factor of 2 scale change in (e). A dashed line along [110] in (e) indicates the electron beam path during the line scan measurements performed for D179.

electron diffraction to be 4930 ± 20 Å, and this corresponds to the position of the MQW-to-capping layer interface. Therefore, as expected from previous studies of highly strained systems,[1,3,10,11] we observe misfit dislocations only at the MQW-to-GaAs interfaces, where the strain is the largest.

Cathodoluminescence images of D38, D18, D92, D155, and D179 are shown in Figs. 3(a)–3(e). The wavelength used for the imaging was $\lambda \approx 950$ nm, and corresponds to the electron-to-heavy hole (e-hh) transition in the MQW samples. The DLDs are evident in each of the images except for D155, the single QW sample [Fig. 3(d)]. The absence of misfit dislocations in the single QW sample is to be expected since the nominal critical thickness of a single $In_{0.2}Ga_{0.8}As$ layer grown on GaAs(100) is ~ 150–200 Å.[12] These images showing DLDs here are similar to luminescence images of thick InGaAs films previously studied.[2–4] A small anisotropy in the DLD density is seen in the CL images of Fig. 3 for dislocations running along both orthogonal [110] directions. This has previously been attributed to the different levels of stress required to generate α and β dislocation cores, and the differences in α and β dislocation propagation velocities.[10,11,13] A DLD linear density of $\sim 10^3$ cm^{-1} is observed. However, it is apparent from the TEM micrograph of Fig. 1(c) that several dislocations can agglomerate close together, resulting in a much higher density than observed with CL. This has also been reported in the studies by Fitzgerald *et al.*[3,4]

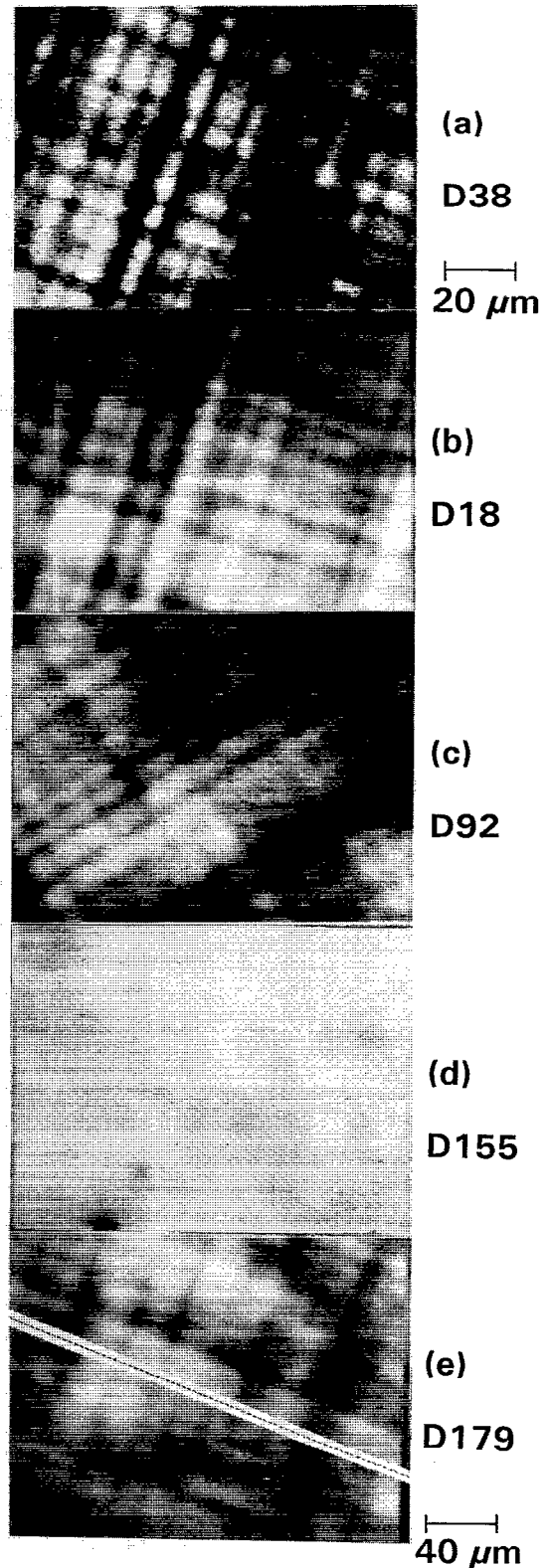In order to further assess the luminescence properties, we examined CL spectra in the wavelength range
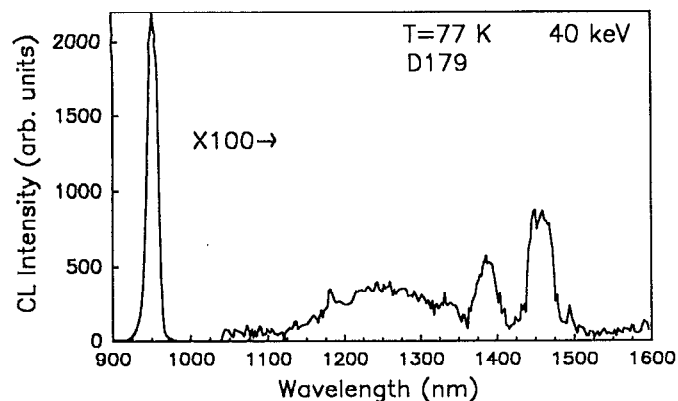
FIG. 4. CL spectrum for MQW sample D179. A factor of $100\times$ change in scale is indicated for the $1000 \lesssim \lambda \lesssim 1600$ nm range. The broad emission bands centered at 1250, 1380, and 1460 nm are thought to be caused by point defects homogeneously dispersed in the MQW structure.
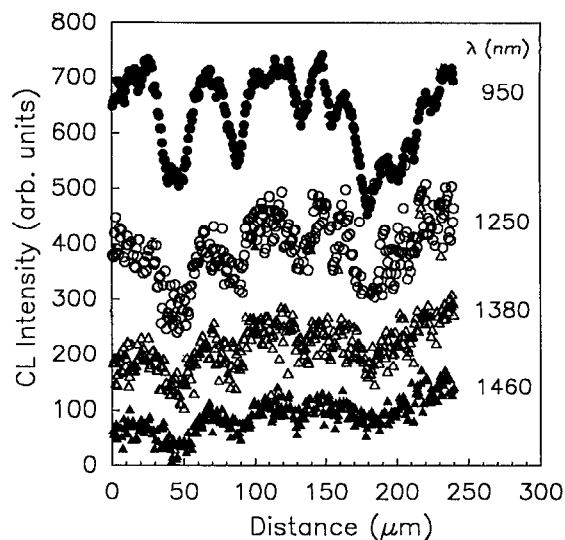

FIG. 5. CL line scans (intensity versus position histogram) for MQW sample D179. The electron beam position is indicated in Fig. 2(e). The peaks and valleys in the $\lambda = 950$ nm scan of the e-hh exciton luminescence correlate with the peaks and valleys of the longer wavelength 1250, 1380, and 1460 nm scans.

$900 \lesssim \lambda \lesssim 1600$ nm. A spectrum of D179, which showed the strongest emission in the $1000 \lesssim \lambda \lesssim 1600$ nm range, is shown in Fig. 4. Four distinct features in the luminescence are observed centered at 950, 1250, 1380, and 1460 nm. The peak at $\lambda = 950$ nm is the e-hh transition. A factor of 100 change in intensity scale between the $\lambda = 950$ nm peak and longer wavelength features is indicated in Fig. 4. The weaker longer wavelength peaks must be related to defects in the MQW structure since the energies are far below the e-hh exciton energy. Impurity-induced emissions tended to be much narrower than the long-wavelength features present in Fig. 4 and were within only a few meV of the InGaAs band edge emission. The broad, quasi-continuous nature of the emissions in Fig. 4 are more suggestive of a structural disorder. Structural defects can generate a continuum of energy levels locally in the band gap, and thus introduce additional radiative and nonradiative recombination channels. Joyce et al.,[5] using photoluminescence, have observed emission in the $1000 \lesssim \lambda \lesssim 1600$ nm range for thick InGaAs films grown on GaAs. These emissions were found to increase markedly when the $In_{0.17}Ga_{0.83}As$ layer thicknesses exceeded the critical thickness, and Joyce et al. concluded that this behavior was due to an increase in interface defects, such as misfit dislocations, beyond the critical thickness.[5] In order to test this hypothesis, we have determined the spatial distribution of all distinct emissions in the wavelength range $900 \lesssim \lambda \lesssim 1600$ nm. We have measured intensity versus position histograms or line scans (see Fig. 5) which quantitatively give the spatial variation in luminescence intensity for the different wavelengths. The line scans for wavelengths of 1250, 1380, and 1460 nm have essentially the same spatial variation as the $\lambda = 950$ nm scan, i.e., peaks and valleys in the longer wavelength scans correspond with peaks and valleys in the $\lambda = 950$ nm scan. This is a surprising result since, from Ref. 5, we would expect the region around the DLDs to yield an enhanced emission rather than the reduced emission at longer wavelengths.

The nature of the dislocation cores (i.e., electronic structure and reconstruction) in strained III-V materials is known to effect the recombination process. The studies of Fitzgerald et al.[3] and Petroff et al.[1] on strained films have shown that 60° dislocations and edge dislocations have different nonradiative recombination rates in the vicinity of these dislocations. It is apparent from the data of Fig. 5 that the nonradiative mechanisms responsible for the reduction in the e-hh exciton luminescence are also responsible for reduction in the $1000 \lesssim \lambda \lesssim 1600$ nm emissions. This results in longer wavelength DLDs spatially correlated with the conventional e-hh exciton DLDs. The origin of the $1000 \lesssim \lambda \lesssim 1600$ nm emissions is, evidently, not *directly* caused by the presence of misfit dislocations and may be due to the presence of point defects. Similar broad and midgap emissions have been observed in thick and heavily strained GaAs films grown on Si which are believed to contain interstitial, antisite, and vacancy defects.[15] In addition, we can not rule out emissions due to the presence of $In_{0.2}Ga_{0.8}As/GaAs$ interfaces (i.e., recombinations involving interface states). Other types of structural defects can also induce midgap emissions. In a separate study of $In_{0.2}Ga_{0.8}As/GaAs$ MQWs grown on patterned GaAs substrates, we have shown that luminescence intensity in the $1000 \lesssim \lambda \lesssim 1200$ nm region is correlated with the density of threading dislocations propagating through the MQW structure.[16] However, our cross-sectional TEM measurements showed no evidence of threading dislocations in the present samples.

To further quantify these results, we have performed line scans for the MQW samples at various accelerating voltages (as shown in Fig. 6 for D179). The electron penetration depth has a known functional dependance on the beam energy. A variation in the beam energy over the range of 10–40 keV results in a corresponding tenfold increase in the penetration depth, R_e, and the peak position,
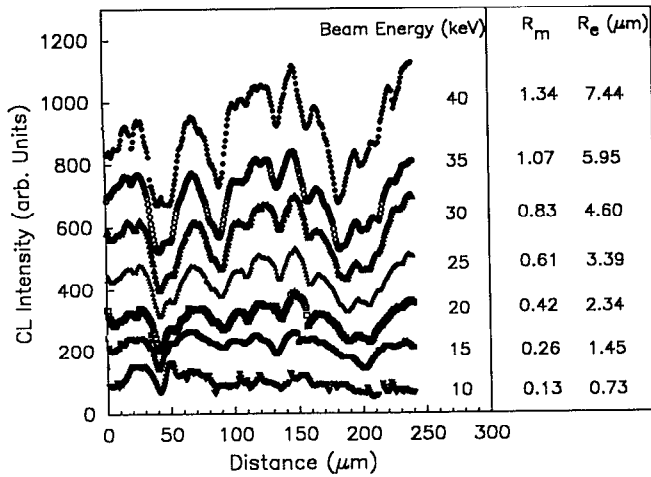
FIG. 6. CL line scans for MQW sample D179 for electron beam energies ranging from 10 to 40 keV. The values of the one-dimensional electron-hole pair density maximum peak position (R_m) and the electron penetration range (R_e) are calculated for a given electron beam energy based on the model of Everhart and Hoff in Ref. 16.

FIG. 7. The normalized standard deviation (σ_N) of the e-hh exciton luminescence line scans for MQW samples. The standard deviation has been normalized to the mean of the exciton luminescence for each line scan. The large magnitude of the variation (see discussion) precludes the possibility of only one QW in each structure being affected by a single dislocation core at the MQW-to-substrate interface.

R_m, of the electron-hole pair density creation function (also known as the "depth-dose" curve) as determined by Everhart and Hoff.[17,18] In Fig. 6, calculated values of R_m and R_e, based on the one-dimensional approach of Everhart and Hoff, are shown next to the beam energy for a given line scan. The minimum probing depth, however, is limited ordinarily by the carrier diffusion length which is typically about 0.5 μm for GaAs.[18] In sample D92, the modulation *nipi* doping will further limit carrier diffusion to negligible values along the growth direction due to the presence of periodic conduction and valence band-edge barriers.[7,8] Thus, by reducing the excitation energy, it is possible to increase the surface sensitivity; that is, the relative fraction of the luminescence arising from recombination in layers closer to the surface.[19] The technique of varying the beam energy to affect the probing depth will facilitate an assessment of possible layer-dependent material variations giving rise to the observed DLDs, as addressed in the following discussions.

A particularly striking result in Figs. 5 and 6 is the large intensity variation seen in the line scan data. The variation of the luminescence in the line scans can be quantified by evaluating the standard deviation of all points shown in a line scan, and normalizing the standard deviation with respect to the mean. In order to reduce the uncertainties due to variation in the signal-to-noise caused by changes in the luminescence signal associated with changing the excitation conditions (current and beam energy) and different sample thicknesses, a cubic spline fit was used to determine the "smooth curve" through each line scan. The normalized standard deviations, σ_N, of the fitted line scans are shown in Fig. 7 for all samples with a beam energy ranging from 10 to 40 keV. A general trend is observed in which σ_N is fairly constant over a large energy range and increases slightly with a decreasing probing depth for energies less than about 20 keV. The total thick-
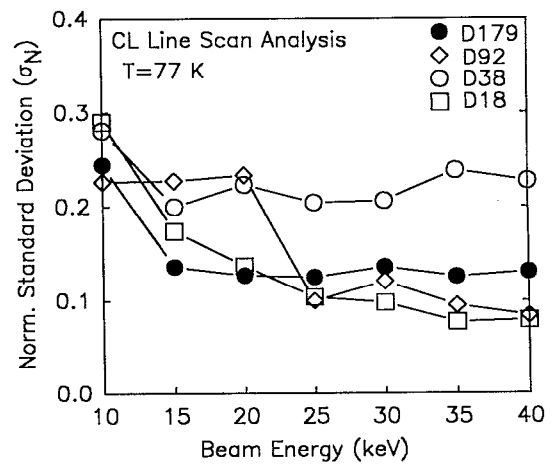
nesses of the MQW region of D179, D92, D38, and D18 are 2.0, 3.7, 0.8, and 2.0 μm, respectively, and a given variation in the probing depth will affect different regions of each sample. From the above TEM results, we know that misfit dislocations occur only in the region at the MQW-to-GaAs substrate and capping layer interfaces. We should expect, therefore, that only recombination in the QW closest to the interface will be disturbed directly by the presence of a misfit dislocation. A predicted σ_N for a 44 MQW structure in which the luminescence from one QW at the interface is completely suppressed by a misfit dislocation, assuming a homogeneous carrier excitation and a simple sinusoidal spatial variation in the luminescence, is $\sigma_N = 0.008$. This is at least an order of magnitude too low to explain the present results of Fig. 7. Instead the magnitude of σ_N and its relative constancy for each sample in Fig. 7 suggest that the nonradiative mechanisms giving rise to DLDs are spread homogeneously throughout all MQWs in each sample, and the effects become slightly more pronounced for more surface sensitive probing conditions.

These results have significant ramifications concerning the origin of the DLDs seen in this and previous studies of thick InGaAs films grown on GaAs. In previous studies, it was simply assumed that the electronic nature of the misfit dislocations were responsible for the creation of competing nonradiative channels.[1,3] In that model, nonradiative minority carrier recombination occurs at the reconstructed dislocation cores as a result of localized band bending in the vicinity of the cores; the density of defect-induced states in the band gap and doping concentration will determine local depletion region sizes. In a similar model involving threading dislocations in $Al_{0.3}Ga_{0.7}As/GaAs$ MQWs, Liu *et al.* proposed that electrically active "kink sites" situated along the dislocation core are responsible for a decrease in luminescence efficiency.[20] However, the present data suggests that carrier recombination at the dis-

location cores is a minor effect in producing the DLDs observed in CL. This can be proven immediately by considering the *nipi* structure of sample D92. The modulation doping will cause electrons and holes to spatially separate for carriers which do not recombine at the location of the $In_{0.2}Ga_{0.8}As$ QWs, and this results in negligible carrier diffusion along the [100] growth direction.[7,8] Therefore, it is apparent that recombination of carriers which are generated more than one MQW period away from the dislocation core would be negligible in this model. The only reasonable explanation for the behavior of σ_N is as follows. The existence of nonradiative recombination centers spread homogeneously in the MQW material away from dislocations is the primary cause of the large variation in the MQW exciton luminescence. The nonradiative centers will evidently compete with the longer wavelength $1000 \lesssim \lambda \lesssim 1600$ nm radiative channels, resulting in the spatial correlation of DLDs imaged at $\lambda \approx 950$ nm with DLDs imaged at longer wavelengths (as illustrated in Fig. 5 for line scans). Dislocation propagation and multiplication such as, e.g., the Hagen-Strunk[21] and surface half-loop nucleation[22] mechanisms are expected to disturb the material located above the dislocations. Heavily dislocated materials, such as that seen in the strained GaAs/Si system are known to contain a significant density of point defects.[15] It is, therefore, likely that a Cottrell atmosphere of point defects left in the wake of dislocation propagation and multiplication coupled with the concomitant epitaxial growth over the vicinities of such propagation are responsible for the observed behavior of σ_N.

IV. CONCLUSION

In conclusion, we have performed TEM and CL imaging and spectroscopy on $In_{0.2}Ga_{0.8}As$/GaAs MQW structures. Cross-sectional and plan-view TEM demonstrate that misfit dislocations are confined to the MQW-to-GaAs interfacial regions. A large variation in the exciton luminescence intensity is observed and is interpreted as due to the presence of nonradiative recombination centers spread homogeneously in the MQW region away from interface misfit dislocations. In addition, these *nonradiative* recombination centers are found to compete with exciton and midgap *radiative* centers at $\lambda \approx 950$ nm and $1000 \lesssim \lambda \lesssim 1600$ nm, respectively, resulting in spatially correlated DLDs for all CL imaging wavelengths. This study introduces a new model describing the origin and nature of DLDs and differs from previous models which have only considered the electronic nature of dislocation cores as the mechanism for inducing DLD radiative contrast in the luminescence imaging of strained InGaAs/GaAs.

ACKNOWLEDGMENT

[1] P. M. Petroff, R. A. Logan, and A. Sauvage, Phys. Rev. Lett. **44**, 287 (1980); J. Microsc. **118**, 255 (1980).

[2] P. L. Gourley, I. J. Fritz, and L. R. Dawson, Appl. Phys. Lett. **52**, 377 (1988).

[3] E. A. Fitzgerald, Y. Ashizawa, L. F. Eastman, and D. G. Ast, J. Appl. Phys. **63**, 4925 (1988); E. A. Fitzgerald, D. G. Ast, P. D. Kirchner, G. D. Pettit, and J. M. Woodall, J. Appl. Phys. **63**, 693 (1988).

[4] E. A. Fitzgerald, G. P. Watson, R. E. Proano, D. G. Ast, P. D. Kirchner, G. D. Pettit, and J. M. Woodall, J. Appl. Phys. **65**, 2220 (1989), and references therein.

[5] M. J. Joyce, M. Gal, and J. Tann, J. Appl. Phys. **65**, 1377 (1989).

[6] L. C. Kimerling and J. R. Patel, Appl. Phys. Lett. **34**, 73 (1979); VLSI Electron. **12**, 223 (1985).

[7] A. Larsson and J. Maserjian, Appl. Phys. Lett. **58** , 1946 (1991).

[8] J. Maserjian, P. O. Andersson, B. R. Hancock, J. M. Iannelli, S. T. Eng, F. J. Grunthaner, K.-K. Law, P. O. Holtz, R. J. Simes, L. A. Coldren, A. C. Gossard, and J. L. Merz, Appl. Opt. **28**, 4801 (1989).

[9] D. H. Rich, A. Ksendzov, R. W. Terhune, F. J. Grunthaner, B. A. Wilson, H. Shen, M. Dutta, S. M. Vernon, and T. M. Dixon, Phys. Rev. B **43**, 6836 (1991).

[10] K. L. Kavanaugh, M. A. Capano, L. W. Hobbs, J. C. Barbour, P. M. J. Maree, W. Schaff, J. W. Mayer, D. Pettit, J. M. Woodall, J. A. Stroscio, and R. M. Feenstra, J. Appl. Phys. **64**, 4843 (1988).

[11] T. George, E. R. Weber, S. Nozaki, T. Yamada, M. Konagai, and K. Takahashi, Appl. Phys. Lett. **59**, 60 (1991).

[12] S. Luryi and E. Suhir, Appl. Phys. Lett. **49**, 140 (1986).

[13] I. Yonenaga and K. Sumino, J. Appl. Phys. **65**, 85 (1989).

[14] A. P. Roth, R. A. Masut, M. Sacilotti, Y. Le Page, G. I. Sproule, and D. F. Mitchell, Superlattices and Microstructures **2**, 507 (1986).

[15] B. A. Wilson, C. E. Bonner, T. D. Harris, M. G. Lamont, R. C. Miller, S. K. Sputz, S. M. Vernon, V. E. Haven, R. M. Lum, and J. K. Klingert, Mater. Res. Soc. Symp. Proc. **91**, 255 (1987). Additionally, in a stress-induced deformation of Si and Ge samples, Schröter, Scheibe, and Schoen [J. Microsc. **118**, 23 (1980)] have argued that variations in the mobility and density of free holes, as determined from Hall measurements, are associated with clouds of point defects which surround dislocations.

[16] D. H. Rich, K. C. Rajkumar, L. Chen, A. Madhukar, and F. J. Grunthaner, Appl. Phys. Lett. **61**, 222 (1992).

[17] T. E. Everhart and P. H. Hoff, J. Appl. Phys. **42**, 5837 (1971).

[18] See, e.g., B. G. Yacobi and D. B. Holt, *Cathodoluminescence Microscopy of Inorganic Solids* (Plenum, New York, 1990).

[19] For an illustration of cathodoluminescence in applications of surface studies see, e.g., L. J. Brillson, R. E. Viturro, J. L. Shaw, and H. W. Richter, J. Vac. Sci. Technol. A **6**, 1437 (1988).

[20] T. Y. Liu, P. M. Petroff, H. Kroemer, and A. C. Gossard, Mater. Res. Soc. Symp. Proc. **145**, 393 (1989); T. Y. Liu, P. M. Petroff, and H. Kroemer, J. Appl. Phys. **64**, 6810 (1988).

[21] W. Hagen and H. Strunk, Appl. Phys. **17**, 85 (1978).

[22] J. W. Matthews, A. E. Blakeslee, and S. Mader, Thin Solid Films **33**, 253 (1976).